

Eco-friendly Preparation and Structural Characterization of Calcium Silicates Derived from Eggshell and Silica Gel

Maroua H. Kaou^{1,2}, Zsolt E. Horváth¹, Katalin Balázsi^{1*} and Csaba Balázsi¹

¹ Institute of Technical Physics and Materials Science, Centre for Energy Research, Konkoly-Thege M. str. 29-33, 1121 Budapest, Hungary

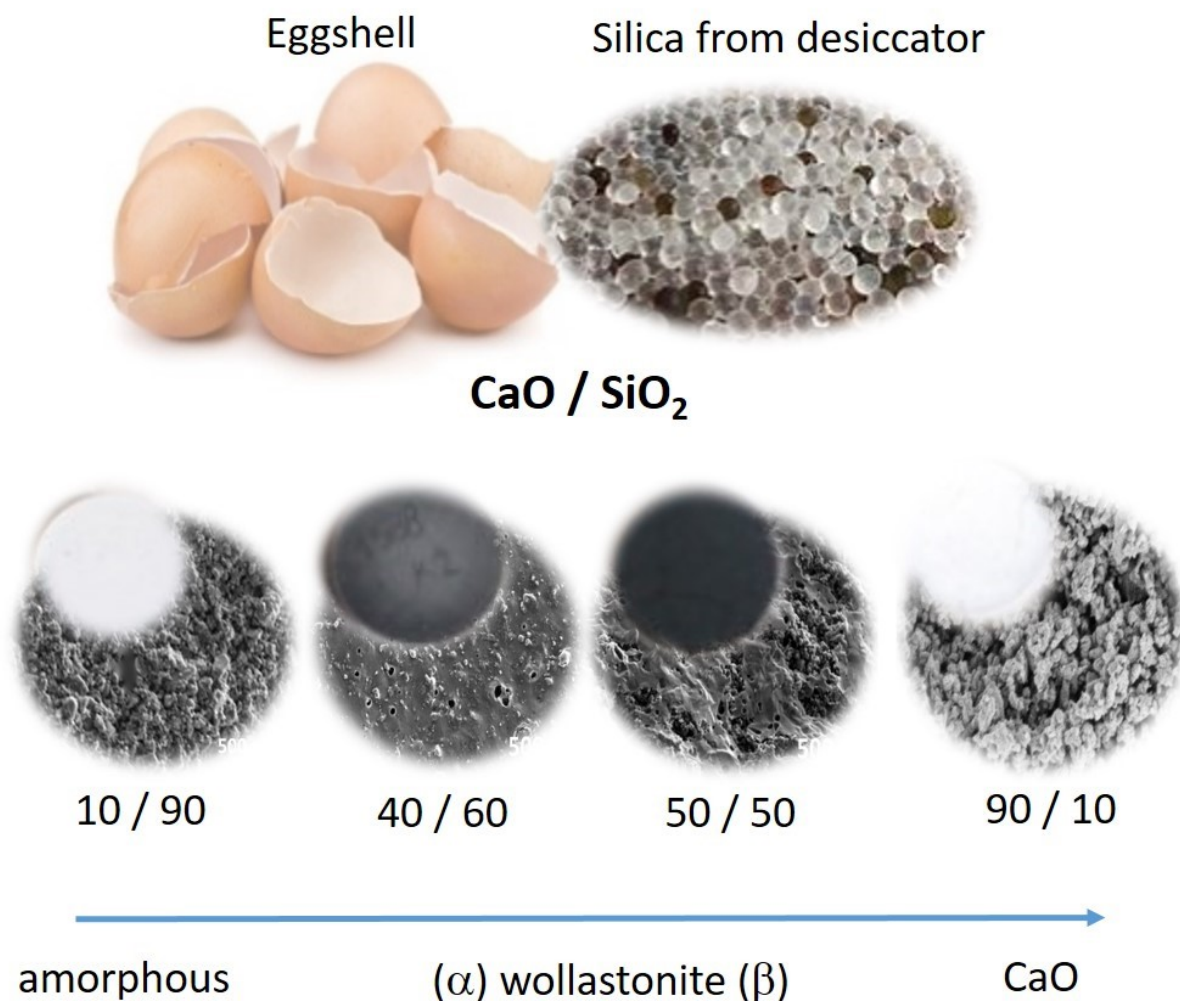
² Doctoral School of Materials Science and Technologies, Óbuda University, Bécsi str. 96/B, 1030 Budapest, Hungary

* Correspondence: author: balazsi.katalin@ek-cer.hu

Abstract: In this work the preparation of calcium-silicate based composites consisting of natural waste from calcium source as eggshell and silica gel from desiccator as a silicon source both presenting alternative materials for cheap preparation of eco-friendly calcium-silicate bioceramics has been investigated. The effect of CaO/SiO₂ ratio on microstructural properties has also been studied. The pseudo-wollastonite formation has been observed in the case of 40 wt.% CaO and 60 wt.% SiO₂ with lowest porosity and highest density 2.6 g/cm³. In the case of 50 wt.% CaO and 50 wt.% SiO₂ the phase transformation from pseudo-wollastonite to wollastonite was observed. Increasing the calcium content caused higher apparent porosity with 19%. It was shown that the development of novel ceramics from reused waste, eggshell or silica can be an optimal solution for low-cost preparation of calcium silicates with potential applications in medicine or cement, food industry.

This article has been accepted for publication and undergone full peer review but has not been through the copyediting, typesetting, pagination and proofreading process, which may lead to differences between this version and the [Version of Record](#). Please cite this article as [doi: 10.1111/ijac.14274](https://doi.org/10.1111/ijac.14274).

This article is protected by copyright. All rights reserved.



Keywords: green processing; eco-friendly approach; eggshell; calcium silicates

1. Introduction

Calcium-silicon (Ca-Si) based materials are important class of bioactive materials because of excellent bioactivity, biodegradability and biocompatibility. Ca and Si ions have drawn huge attention in the biomedical field due to their direct contribution in many biological processes as in controlling and enhancing cellular responses for bioceramics. Bioactive glasses and bioceramics have been widely investigated for their beneficial applications in bone repairing and ability to bond to the surrounding tissues through the formation of an apatite layer on the surface [1, 2]. These ceramics have been developed and some of them has been already used in the clinic in order to enhance the properties such the low fracture toughness, the high solubility [3-8]. On the other hand, calcium silicate is a type of ceramic material that can be applied in different areas as an anticaking agent in the food industry, agriculture, ceramic, cement and in the building industry, due to their unique

properties from lightweight, low thermal conductivity. Several studies have been carried out to demonstrate the importance of the dissolution products of bioactive silicate-based ceramics in promoting osteoblast proliferation and differentiation [3, 9-12]. *Li et al.* demonstrated the significant improvement of the immunosuppressive function of human bone marrow mesenchymal stem cells (HBMSCs) [12]. Calcium silicate activated HBMSCs showed stronger stimulatory effects on cell phenotype polarization of macrophages than calcium silicate ionic products since they can directly interact with macrophages [12].

Due to CaO / SiO₂ ratio several calcium-silicate can be identified, such as CaSiO₃, Ca₂SiO₄, Ca₃SiO₅, and Ca₃Si₂O₇ [3, 9]. Monocalcium silicate (CaSiO₃) is presented in two polymorphic forms; wollastonite (β -CaSiO₃) and pseudo-wollastonite (α -CaSiO₃) [10]. Five different crystal phases are denoted for dicalcium silicate (Ca₂SiO₄); γ phase stable at room temperature; thermodynamically unstable β phase and high temperature stable α , α' L, α' H. On the other hand, tricalcium silicate (Ca₃SiO₅) stable phase exists only between 1250 °C and 1900 °C. Up to 1900 °C, Ca₃SiO₅ will decompose to Ca₂SiO₄ and calcium oxide (CaO) [3, 10]. Both of Ca₂SiO₄ and Ca₃SiO₅ have been already applied in dentistry as the main components of the Portland and MTA (Mineral Trioxide Aggregate) cements. *Obeid M.M.* synthesized the wollastonite (CaSiO₃) by the solid state reaction method at a temperature range of 1050-1250°C from local raw materials, e.g. silica sand and limestone [13]. β -wollastonite was obtained at 1050°C and transformed to pseudo-wollastonite (α -CaSiO₃) at 1150°C due to the presence of B₂O₃.

The synthesis method can influence the biological behaviors, the porosity, precursors, sintering temperature and the glass composition as well. One of the most used method for the calcium silicate preparation is the sol-gel method. It can offer high homogeneity and purity compared to the quench melting methods. *Wajda et al.* studied the effect of the preparation method on the structure and the properties of the CaO-SiO₂ system [2]. It has been shown that both melt-derived and sol-gel glasses were fully amorphous, the gel-derived glass had a more polymerized structure compared to the melt derived one [2]. In the case of melt-derived calcium silicate (30 mol% CaO and 70 mol% SiO₂), glassy spherical droplets (inclusions) in glassy matrix was observed.

Ernawati L. et al. studied the environmentally friendly solid-state method to prepare mesoporous wollastonite (calcium-silicate, CaSiO₃) based composite adsorbent from chicken eggshells and SiO₂ powder as starting materials [14]. The wollastonite phase was obtained at a CaCO₃/SiO₂ molar ratio of 1:5 and 2:5 and calcined at 1100°C for 4 h. The purity of the raw materials and molar ratio of CaCO₃/SiO₂ affect the final product of CaSiO₃ materials

with irregular shape morphology, specific surface area of $3.053 \text{ m}^2 \text{ g}^{-1}$ and a small pore diameter of 1.52 nm. Higher molar ratios of CaCO_3 produced CaSiO_3 with quartz and olivine phases which is more suitable for wastewater treatment application. *Yudha S.S.* et al. described the synthesis of calcium silicate derivatives using natural resources such as eggshell (ES) for calcium and oil palm leaves (OPL) for silica [15]. They successfully synthesized via the solid-state reaction the powder materials containing calcium silicate derivatives, mainly Ca_2SiO_4 and a small amount of CaSiO_3 . Their results demonstrate that the concentration of the precursors has an effect on the micrometer-sized particles irregular surface morphology and crystallinity of the final powders. *Palakurthy S.* et al. used the eggshells and rice husk ash bio-wastes as sources of calcium oxide (CaO) and silica (SiO_2) for preparation of $\text{SiO}_2\text{-CaO-Na}_2\text{O}$ bio-glass [16]. Bioglass samples were obtained by melt-quenching technique and displayed highly irregular-shape morphology with the particle size distribution ranging from 1 to 20 μm . Hence, their cytocompatibility test showed that the synthesized $\text{SiO}_2\text{-CaO-Na}_2\text{O}$ bio-glass had no biological cell toxicity and consequently it can play a considerably active role in biomedical applications.

The aim and novelty of the presented study has been to investigate the preparation of calcium-silicate based composites consisting of natural waste having calcium source as eggshell and silica gel from desiccator as a silicon source both presenting alternative materials for cheap preparation of eco-friendly calcium-silicate bioceramics. Nowadays, clinical demands related to novel calcium silicates with possible usage in wound healing and tissue regeneration for public are increasing with the increasing in number and aging of population. The development of novel ceramics from reused waste namely eggshell or silica from chemical laboratories can be an optimal solution for low-cost materials in comparison to materials elaborated by synthetic ways representing increasing risks in respect to green environment.

2. Materials and Methods

2.1. Preparation of the starting materials, powder mixtures, and porous ceramics

Calcium silicates have been successfully prepared using an eco-friendly source represented in chicken eggshells and SiO_2 from desiccators. The preparation steps are shown in Fig.1. The eggshells – as calcium source - have been rinsed, dried, and crushed, and then subjected to heat treatment in the air at 900 °C for 12h. The silica (SiO_2 , Chemolimpex, “A” quality 1-6 mm, Budapest, Hungary) has been prepared from silica gel (~100 gr a batch) by

intensive ball milling (Fritsch GmbH) for 3h in dry conditions using alumina bowls (500 ml) and 10 balls of alumina (each one has about 10 mm in diameter).

Different CaO/SiO₂ ratios have been applied during the preparation of powder mixtures using attrition milling, among all of them the following ratios: 10C90S, 40C60S, 50C50S, and 90C10S have been chosen due to their different compositions and structures (Tab. 1). The powder mixtures (~100 gr a batch) have been milled in 100 g ethanol with zirconia balls (1 mm in diameter). The milling process has been carried out in a high efficient attritor mill (Union Process, type 01-HD/HDDM) at 2000 rpm for 3h with adding the PEG (Poly Ethylene Glycol) as a pressing aid about 10 g in the last half hour of milling and changing the rotation speed to 500 rpm. The mixtures have been dried at 151 °C and sieved with a mesh size of 100 µm. The powder mixtures have been pressed into disc-shaped green samples (about 17 mm in diameter) in dry conditions at room temperature, under mechanical pressure of 18 MPa. The green samples have been heat treated in the air at 800 °C for 1h.

2.2. Characterization methods

The phase composition of powders and final ceramic discs have been determined by X-ray diffractometry (AXS D8 Discover diffractometer with Cu K radiation). Diffrac.Eva software has been used for identification and evaluation of the crystalline phases. The morphological properties of the powders have been performed by a scanning electron microscopy (SEM, LEO (ZEISS) 1540 XB field emission scanning electron microscope) for final ceramics by a Scanning electron microscopy (SEM, Thermo Scientific, Scios2, Waltham, MA, USA). Energy-Dispersive X-ray Spectrometry (Oxford Instrument EDS detector X-Maxn, Abingdon, UK) carried at SEM has been used for the determination of the elemental composition.

The apparent and bulk densities of the ceramic discs have been measured using Archimedes method (Eq. 1 and 2 respectively) with water as the immersion medium [17]. The pressed and heat treated samples with high surface porosity have been immersed into water for at least 3 days to ensure the total filling of the pores. Further, the apparent porosity of the samples has been calculated according to (Eq. 2) [18].

$$\text{Apparant density} = \frac{\text{wt. of dry sample}}{\text{wt. of sample after soaking in water} - \text{wt. of soaked immersed sample}} \times \rho_{\text{water}} \quad (1)$$

where ρ_{Water} corresponds to water density at room temperature.

Further, the apparent porosities of the composites were calculated according to Equation (2).

$$\text{Apparent porosity} = \frac{\text{wt. of soaked sample} - \text{wt. of dry sample}}{\text{wt. of soaked sample} - \text{wt. of immersed sample}} \cdot 100 \quad (2)$$

The measurements of the surface roughness of the heat-treated ceramic discs were performed with Digital Microscope (KEYENCE, VHX-950F, Japan).

3. Results and discussion

3.1. Structural study of the starting materials

The eggshells and SiO₂ gel have been used as starting materials. The eggshells have been calcinated at 900°C for 12h. Morphological investigations confirmed the regular micrometer sized morphology of rod-like particles (Fig. 2a). The average length of rods are 3 μm. Whereas the milled silica gel after 3h milling exhibited a coarse morphology with uniform geometry and grain size (Fig. 2b). The grain size distribution has been observed between few ten nanometers and 1 μm.

The phase analysis of starting materials are shown in Fig. 3a. The calcined eggshells presented two main phases; calcium oxide (CaO) and calcium hydroxide (Ca(OH)₂). The presence of Ca(OH)₂ in structure is justified by fast CaO transformation to Ca(OH)₂ in presence of atmospheric humidity as a result of the moisture absorption as shown in earlier studies by Balázsi et al. [19], Tangboriboon et al. [20].

The XRD diffractogram exhibit the peaks of Fcc CaO (JCPDS 01-082-1690) at 2θ = 32.243, 37.402, 53.929, 64.242° and hexagonal Ca(OH)₂ (JCPD 00-044-1481) at 2θ = 18.008, 34.102, 47.121, 50.813°. Ca(OH)₂ can be formed due to the interaction of CaO with water vapour on the air [19,20]. The milled silica (for 3h) was confirmed to have an amorphous phase - no characteristic peaks have been detected (Fig. 3a).

Calcinated eggshells consisted of calcium (Ca), oxygen (O) and some trace elements as magnesium (Mg) and strontium (Sr) (Fig. 3b). These elements are residuals from eggshell raw material and preparation process [21]. Mg has been known as one of the cationic substitutes for calcium in the calcium phosphate lattice and carbonate or fluoride are simultaneously incorporated together with magnesium as paired substitutions [22,23]. In the case of silica, silicon and oxygen were obtained. It was confirmed that the milling process has been done without any contamination.

3.2. Structural investigation of powder mixtures and final ceramic discs

The different powder mixtures have been prepared from starting materials (Tab. 1). Their morphological study is shown in Fig. 4. As we can see, there is a noticeable effect of the milling process on the morphology of CaO, due to the grinding; the regular micrometer sized morphology of rod-like particles has disappeared.

On the other hand, the powders exhibited a coarse morphology and a finer granular structure. The difference is strongly correlated to CaO/SiO₂ ratio. The powder mixture is consisting of 10 wt.% CaO-Ca(OH)₂ and 9 times higher amount of SiO₂ consisted of 1 μm sized calcium oxide based grains covered by fine grains SiO₂ (Fig. 4a). The average grain size of powder mixture decreased with increasing of CaO-Ca(OH)₂ content (Fig. 4a-d). The milling process had a multiple effect on the dispersibility of SiO₂ in CaO matrix, to the morphology of the grains of the powder mixtures (Fig. 4) and did cause slight phase changes as it will be well discussed in the next section of the XRD analysis of the powders (Fig. 6a).”

The SEM-EDS mapping and spectra in Fig. 5 and Tab. 2 show the presence of Ca, Si, O, Mg and Na, P elements (at very low amounts) for all powder mixtures. However, the element P was not detected for the composition 10C90S, this could be explained by the small amount of calcium oxide (CaO) present in the mixture. We can observe the difference in the intensity and the weight percent (Wt.%) of each element vary with the variance of CaO and SiO₂ in the mixture. On the other hand, the detection of the Carbon (C) element was due to the carbon tape used in the fixation of the powders on the sample holder in order to perform the SEM-EDS analysis.

The table below presents the EDS spectra with the atomic and weight percentages of elements for each powder.

The EDS results of calcium-silicate powder mixtures show the explicit increase of Ca (left) and decrease of Si (right) consistent with the CaO/SiO₂ ratio in the order of starting from the up to bottom 10/90, 40/60, 60/40 and 90/10 (Fig. 5 and Tab. 2).

Comparison of the phase composition of the powder mixtures: 10C90S, 40C60S, 50C50S, and 90C10S have been performed by XRD (Fig. 6a). In all cases, the hexagonal Ca(OH)₂ (JCPD 00-044-1481) was detected. The intensity of these peaks increased with the increase of the Ca(OH)₂ amount in the composition. It can be noticed the presence of a minor Ca₂SiO₄ phase (JCPD 00-033-0302) at 2θ= 29.268° that can be evolve during high intensive

milling process in the composition 90C10S. Whereas for the composition 10C90S where the silica amount is high, the compound tends to have an amorphous phase. *Meiszterics A. et al.* developed the calcium silicate systems by sol-gel methods—varying the synthesis conditions. They showed that the amorphous silica network decomposed, the bond system of Ca silicate started developing, a crystalline phase disappears, and a new one forms. Considering these changes, the required temperature of heat treatments is 600 °C [24]. In present work, the heat treatment at 800°C for 1h was applied and it induced the phase (Fig. 6b) and morphological (Fig. 7) changes as well.

10 wt.% calcinated eggshell and 90 wt.% milled SiO₂ composition resulted the fully amorphous material (10C90S, Fig. 6b). The increasing of Ca(OH)₂ to 40 wt.% caused the crystallization in pseudo-wollastonite (α -CaSiO₃), JCPD 01-074-0874) structure (40C60S, Fig. 6b). The phase evolution is strongly dependent on the Ca(OH)₂ / SiO₂ ratio. The phase transformation from hex Ca(OH)₂ to pseudo-wollastonit, wollastonit (β -CaSiO₃, JCPD 00-042-0547) and triclinic Ca₃(SiO₄)O (JCPD 01-070-1846) have been observed for Ca(OH)₂ / SiO₂ ratio 50/50 (50C50S, Fig. 6b). In the case of 90 wt% Ca(OH)₂ all free calcium ions were bonded by oxygen created the fcc CaO phase. The minor silica has been crystalized in triclinic Ca₃(SiO₄)O and the lines of minor monoclinic Ca₂SiO₄ phase can be also recognized in the $2\theta = 28-32^\circ$ range.

The structural study of the heat treated pressed samples showed different morphologies depending on composition (Fig. 7). The phase composition 10C90S showed a fine structure (Fig. 7a) like amorphous which was confirmed by XRD, respectively (Fig. 6b). An increase in the calcium-based amount about 40 %wt. to the previous composition led to a high melted and densified microstructure with the presence of porosities on the surface, their sizes are in the range of few hundred nanometers (40C60S, Fig. 7b).

In the case of 50C50S with pseudo- and wollastonite phases, the microstructure with 100 nm grain size in average has been detected (Fig. 7c). High 90 wt.% fcc CaO content (90C10S) revealed to have a porous microstructure with a coarse refined morphology resulting in 5 times bigger grains than in the case of 50/50 ratio (Fig. 7d).

The apparent density measurements are illustrated in Fig. 8. The highest density value can be achieved at 40/60 ratio (2.639 g/cm³) followed by 50/50 (2.037 g/cm³) and 10/90 (1.509 g/cm³). In the case of 90/10 due to extremely high porosities, no density measurement was observed. It can be seen that the values of the apparent densities increase when the

weight ratios CaO/SiO₂ increase from 10/90 up to 40/60 and then go down (Fig. 8). The reduction of the apparent density when the weight ratios CaO/SiO₂ increase up to 50/50 in the structure of composites could be ascribed to the decrease in the specific surface area of composites. *Suda et al.* [25] have observed a linear relationship between density and Ca/Si ratio in the case of cementitious materials based on C-S-H. It was demonstrated that the Ca/Si ratio has an effect on both the density and the specific area of the cementitious C-S-H. As the density increases with the increase in the molar ratio Ca/Si, the specific surface area will decrease (inverse relationship between the specific area and the Ca/Si molar ratio) [25,26]. Similar structural results were observed by *Mabah D.E.T et al.* [26]. Their work investigated the influence of the molar ratio CaO/SiO₂ (0, 0.4, 0.6, 0.8, 1.0 and 1.2) contained in the sustainable composites on the microstructural properties using sodium waterglass from rice husk ash and commercial sodium waterglass as chemical reagents. They confirmed that the lower amorphous calcium silicate hydrate content is related to the lower amount of SiO₂ in the structure of microcomposite. On the other hand, the reduction of the apparent density from cca. 2 to 1.65 g/cm³ was observed [26]. In their work, the molar ratios CaO/SiO₂ increase from 0.4 to 1.2 in the structure of microcomposites could be ascribed to the decrease of the specific surface area of microcomposites [26].

In their study a similar trend in apparent density - CaO/SiO₂ relation was observed, thus the apparent density of (Ca, Na)- poly (sialate-siloxo) networks increase when the molar ratios CaO/SiO₂ in the structure of composites increase from 0 to 0.4 and then decrease. *Gallucci E. et al* studied the effect of temperature on the microstructure of calcium silicate hydrate when the weight loss due to decarbonation of calcite was taken as the loss from 600 to 780 °C [27]. Calcium silicate prepared from eggshells and silica gel demonstrated differences in the lost weight of the pressed ceramics before and after heat treatment at 800°C for 1h (Tab. 3). In our case, the composition (Ca/Si ratio) effected the final weight loss of materials. The highest weight loss has been observed for CaO/SiO₂ ratio 40/60 (Tab. 3).

Calcium silicate with 90 wt.% CaO and 10 wt.%SiO₂ (90C10S) increased in size after heat treatment. This effect was caused by morphology and interconnected open porosities (Fig. 7d). It was demonstrated the direct effect of CaO/SiO₂ ratio on structure, porosity and weight loss.

The porosity differed widely, likely due to composition and the particle size differences in the heat treated calcium silicate (Tab.3). *G.A. Gandolfi et al.* developed the calcium silicate-based biomaterials with apparent porosity ~29.36% [28]. M.M. Salmani et al. also

fabricated a porous scaffold made of three components with porosity 33%–22% [11]. The volume of porosity can be changed by composition. In the case of CaO/SiO₂ ratio 40/60 no porosities were measured. 32% was obtained for CaO/SiO₂ ratio 10/90 (Tab.3). On the other hand, CaO/SiO₂ ratio 90/10 was presented as extremely porous material.

Good biocompatibility and bioadhesion of these tailor-made surfaces are attained by an advantageous combination of surface roughness and chemistry [29]. It is well known that a bone cross-section from cancellous to cortical bone is non-uniform in porosity and pore dimensions. Thus, in various attempts to mimic the porous structure of bones, calcium silicate and phosphate bioceramics are designed with graded porosity and roughness from macro- to nanoscale [29,30]. The roughness of the surfaces of calcium silicates can be characterized in the range of 20 – 87 μm (Fig. 9). The lowest roughness ~ 20.07 μm has been measured for CaO/SiO₂ ratio 40/60 (40C60S) and got completely smooth surface (Fig. 9b). This result showed good agreement with density, apparent porosity (Tab. 3) measurements and morphological study (Fig. 7b), respectively.

4. Conclusions

The development of novel bioceramics from waste can be an optimal solution for the low-cost materials with respect to green environment. The natural waste, namely eggshell and silica gel from desiccator, as an alternative form for cheap preparation of eco-friendly calcium silicate ceramics has been investigated. The versatile heat treatment and milling were applied in this study. Calcium silicates with different CaO/SiO₂ ratio have been prepared. The effect of CaO/SiO₂ ratio on microstructural properties has been studied. The 10/90 ratio resulted in amorphous structure with low density ~1.2 g/cm³. The pseudo-wollastonite have been observed in the case of 40 wt.% CaO and 60 wt.% SiO₂ with zero porosity and highest density 2.6 g/cm³. Increasing the calcium content induced the phase transformation from pseudo- to wollastonite showing higher apparent porosity ~ 19%. The CaO/SiO₂ ratio 90/10 resulted mainly fcc CaO. The 40wt.% calcinated eggshell with 60 wt.% milled silica prepared at 800°C for 1h can be the optimal composition for potential bone reconstruction. Future works will be related to thorough biocompatibility investigation of the realized calcium silicates by cost efficient and eco-friendly way.

Acknowledgments: The authors sincerely thank to colleagues from Centre for Energy Research ELKH, Viktor Varga for helping us in carrying out the sample preparation, Noémi

Szász and Levente Illés for technical help in the SEM-EDS analysis of the samples, Dr. Dheeraj Varanasi for optical microscopy measurements.

References

- [1] B. Zagrajczuk, M. Dziadek, Z. Olejniczak, K. Cholewa-Kowalska, M Laczka, Structural and chemical investigation of the gel-derived bioactive materials from the $\text{SiO}_2\text{-CaO}$ and $\text{SiO}_2\text{-CaO-P}_2\text{O}_5$ systems, *Ceram. Int.* 43 (2017) 12742-12754.
<http://dx.doi.org/10.1016/j.ceramint.2017.06.160>
- [2] A. Wajda, M. Sitarz, Structural and microstructural comparison of bioactive melt-derived and gel-derived glasses from CaO-SiO_2 binary system, *Ceram. Int.* 44 (2018) 8856-8863.
<https://doi.org/10.1016/j.ceramint.2018.02.070>
- [3] G.C. Wang, Z.F. Lu, H. Zreiqat, Bioceramics for skeletal bone regeneration. In: K Mallick. (ed) *Bone Substitute Biomaterials*. 1st ed United Kingdom: Woodhead Publishing (Elsevier), 2014, 180-216. DOI : 10.1533/9780857099037.2.180
- [4] M. Catauro, A. Dell’Era, S. Vecchio Cipriotti, Synthesis, structural, spectroscopic and thermoanalytical study of sol-gel derived $\text{SiO}_2\text{-CaO-P}_2\text{O}_5$ gel and ceramic materials, *Thermochim. Acta* 625 (2016) 20-27. <https://doi.org/10.1016/j.tca.2015.12.004>
- [5] J.R. Jones, Reprint of: Review of bioactive glass: From Hench to hybrids, *Acta Biomater.* 23 (2015) S53-S82. <http://dx.doi.org/10.1016/j.actbio.2015.07.019>
- [6] S. M. Rabiee, N. Nazparvar, M. Azizian, D. Vashae, L. Tayebi, Effect of ion substitution on properties of bioactive glasses: A review, *Ceram. Int.* 41(2015) 7241-7251.
<https://doi.org/10.1016/j.ceramint.2015.02.140>
- [7] M. Catauro, F. Bollino, R.A. Renella, F. Papale, Sol-gel synthesis of $\text{SiO}_2\text{-CaO-P}_2\text{O}_5$ glasses: Influence of the heat treatment on their bioactivity and biocompatibility, *Ceram. Int.* 41 (2015) 12578-12588. <http://dx.doi.org/10.1016/j.ceramint.2015.06.075>
- [9] S.K.S. Hossain, P.K. Roy, Development of sustainable calcium silicate board:Utilization of different solid wastes, *Bol. de la Soc. Esp. de Cerám.* 5 (8) (2019) 274-289.
<https://doi.org/10.1016/j.bsecv.2019.06.003>
- [10] P. Srinath, A. K. Azeem, V. Reddy, Review on calcium silicate-based bioceramics in bone tissue engineering, *Int. J. Appl. Ceram. Technol.* 17(2020)2450-2464. DOI: 10.1111/ijac.13577

- [11] M. M. Salmani, M. Hashemian, A. Khandan, Therapeutic effect of magnetic nanoparticles on calcium silicate bioceramic in alternating field for biomedical application, *Ceram. Inter.* 46 (2020) 27299-27307. <https://doi.org/10.1016/j.ceramint.2020.07.215>
- [12] H. Li, W. Wang, J. Chang, Calcium silicate enhances immunosuppressive function of MSCs to indirectly modulate the polarization of macrophages, *Regen. Biomat.*, 8(6) (2021) rbab056. doi: 10.1093/rb/rbab056
- [13] M.M. Obeid, Crystallization of Synthetic Wollastonite Prepared from Local Raw Materials, *Int. J. Mat. Chem.* 4(4) (2014) 79-87. doi:10.5923/j.ijmc.20140404.01
- [14] L. Ernawati, R.A. Wahyuono, A.D. Laksono, A. Ningrum, K. Handayani, A. Sabrina, Wollastonite (CaSiO₃)-based Composite Particles for Synthetic Food Dyes (Brilliant Blue) Removal in Aquatic Media: Synthesis, Characterization and Kinetic study, *IOP Conf. Series: Materials Science and Engineering* 1053 (2021) 012001. doi:10.1088/1757-899X/1053/1/012001
- [15] S.S. Yudha, A. Falahudin, N.H. Mohd Kaus, S. Thongmee, S. Ikram, A. Asdim, Preliminary Synthesis of Calcium Silicates using Oil Palm Leaves and Eggshells, *Bull Chem. Reaction Eng. & Catal* 15 (2) (2020) 561-567. <https://doi.org/10.9767/bcrec.15.2.7591.561-567>
- [16] S. Palakurthy, K.V. Reddy, S. Patel, P.A. Azeem, A cost effective SiO₂-CaO-Na₂O bio-glass derived from bio-waste resources for biomedical applications, *Progr Biomat.* 9 (2020) 239-248. <https://doi.org/10.1007/s40204-020-00145-0>
- [17] S. Lamnini, Z. Károly, E. Bódis, K. Balázs, C. Balázs, Influence of structure on the hardness and the toughening mechanism of the sintered YSZ/MWCNTs composites, *Cer. Int.* 45 : 4 (2019) 5058-5065, <https://doi.org/10.1016/j.ceramint.2018.11.207>
- [18] B. Berger, The Importance and Testing of Density / Porosity / Permeability / Pore Size for Refractories, in: *South. African Inst. Min. Metall. Refract.*, (2010) 111-116.
- [19] C. Balázs, F. Wéber, Z. Kövér, E. Horváth, C. Németh, Preparation of calcium-phosphate bioceramics from natural resources, *J. Eur. Cer. Soc.*, 27 : 2-3 (2007) 1601-1606. doi:10.1016/j.jeurceramsoc.2006.04.016
- [20] N. Tangboriboon, R. Kunanuruksapong, A. Sirivat, Preparation and properties of calcium oxide from eggshells via calcination, *Materials Science-Poland*, 30 (4), (2012) 313-322. DOI: 10.2478/s13536-012-0055-7
- [21] A. Lesbani, P. Tambah, R. Mohadi, F. Riyanti, Preparation Calcium Oxide (CaO) from Chicken Eggshells, *Indo. J. Chem.* 13/2 (2013) 176. <http://dx.doi.org/10.22135/sje.2016.1.2.32-35>

- [22] K. Balázs, H.-Y. Sim, J.-Y. Choi, S.-G. Kim, C.-H. Chae and C. Balázs, Biogenic nanosized hydroxyapatite for tissue engineering applications, *Proceedings of the 5th Eur. Conf. Int. Fed. Med. Biolog. Eng.* 37 (2011) 996-999. DOI: 10.1007/978-3-642-34197-7_50
- [23] RZ. LeGeros, Calcium phosphates in oral biology and medicine, *Monogr Oral Sci.* 15 (1991)1-201. PMID: 1870604.
- [24] A. Meiszterics, K. Sinko, Sol-gel derived calcium silicate ceramics, *Colloids and Surfaces A: Physicochem. Eng. Aspects* 319 (2008) 143–148. <https://doi.org/10.1016/j.colsurfa.2007.08.021>
- [25] Y. Suda, T. Saeki, T. Saito, Relation between chemical composition and physical properties of C-S-H generated from cementitious materials, *J. Adv. Concr. Technol.* 13 (2015) 275–290. doi:10.3151/jact.13.275
- [26] D.E.T. Mabah, H. K. Tchakout, D. Fotio, C.H. Rüscher, E. Kamseu, M.C. Bignozzi, C. Leonelli, Influence of the molar ratios CaO/SiO₂ contained in the sustainable microcomposites on the mechanical and microstructural properties of (Ca, Na)-poly(sialate-siloxo) networks, *Mat. Chem. & Physics* 238 (2019) 121928., <https://doi.org/10.1016/j.matchemphys.2019.121928>
- [27] E. Gallucci, X. Zhang, K.L. Scrivener, Effect of temperature on the microstructure of calcium silicate hydrate (C-S-H), *Cement and Concrete Research* 53 (2013) 185–195. <http://dx.doi.org/10.1016/j.cemconres.2013.06.008>
- [28] M. G. Gandolfi, F. Siboni, T. Botero, M. Bossù, F. Riccitiello, C. Prati, Calcium silicate and calcium hydroxide materials for pulp capping: biointeractivity, porosity, solubility and bioactivity of current formulations, *J Appl Biomater Funct Mater* 13 (1)(2015) 43-60. DOI: 10.5301/jabfm.5000201
- [29] N. Abbasi, S. Hamlet, R.M.Love, T. Nguyen, Porous scaffolds for bone regeneration, *Journal of Science: Advanced Materials and Devices* 5 (1) 2020 pp. 1-9, <https://doi.org/10.1016/j.jsamd.2020.01.007>
- [30] M. Prakasam, J. Locs, K. Salma-Ancane, D. Loca, A. Largeteau, L. Berzina-Cimdina, Fabrication, Properties and Applications of Dense Hydroxyapatite: A Review, *J. Funct. Biomater.* 2015, 6(4), 1099-1140; <https://doi.org/10.3390/jfb6041099>

Figure captions

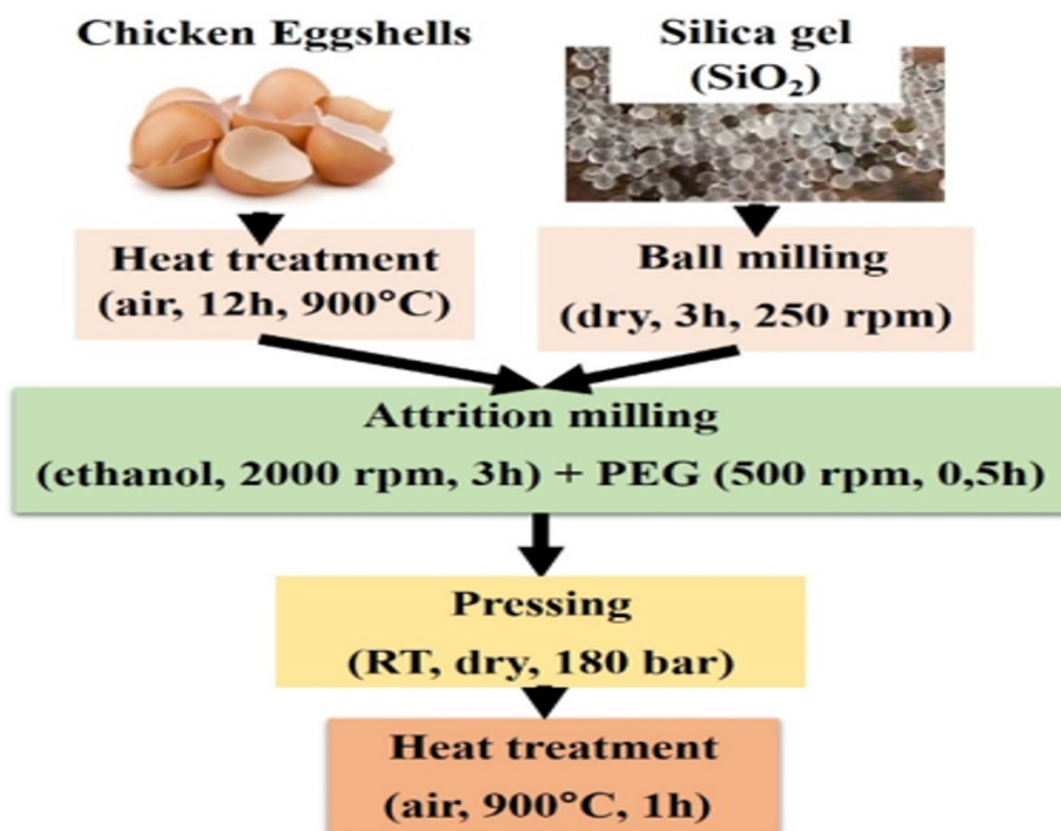
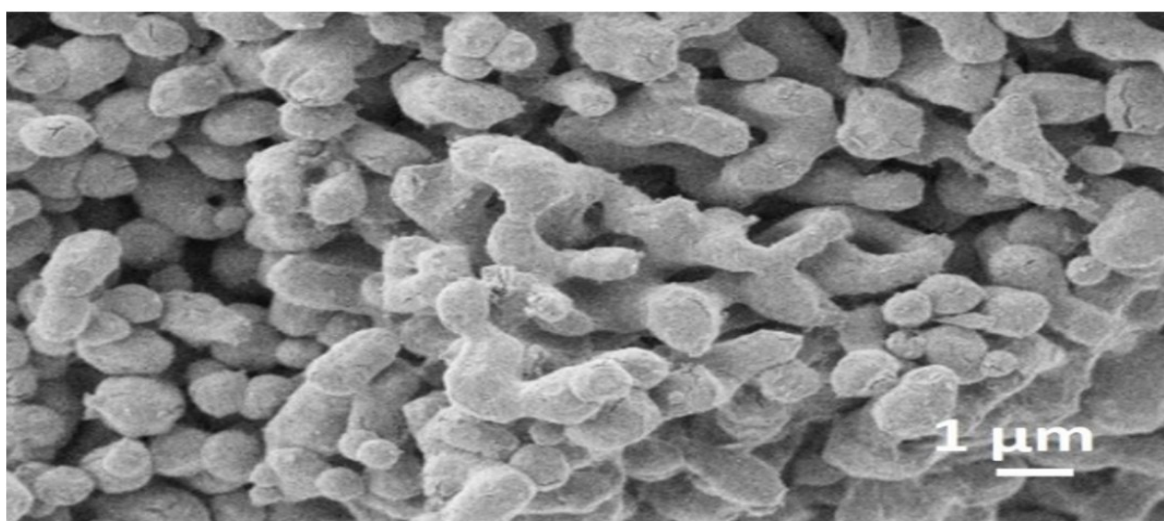


Figure 1. Schematic view of detailed preparation steps.



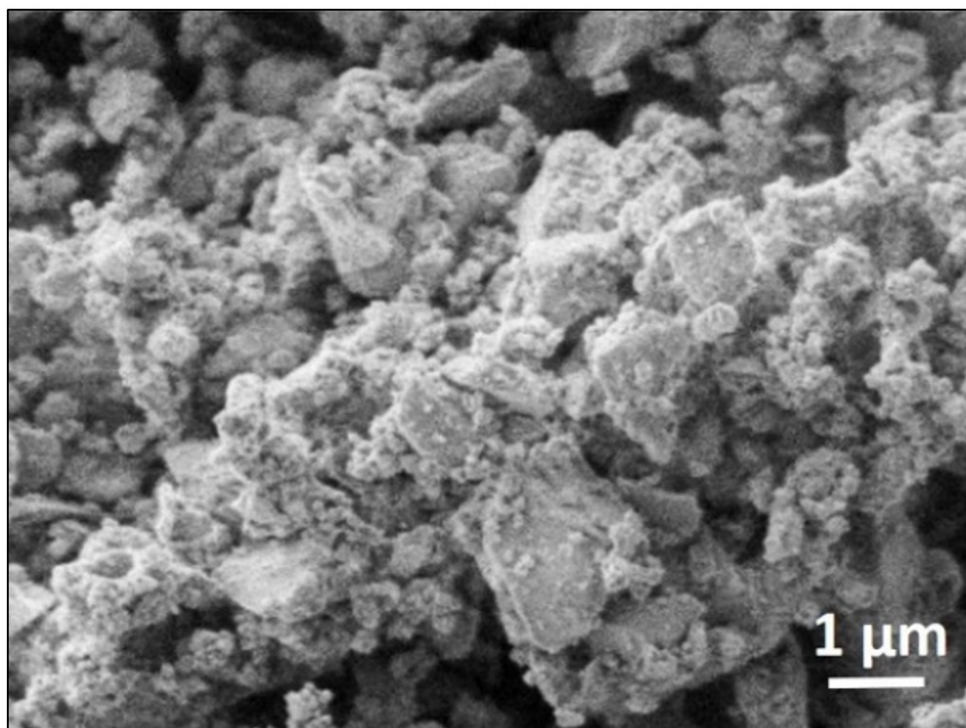
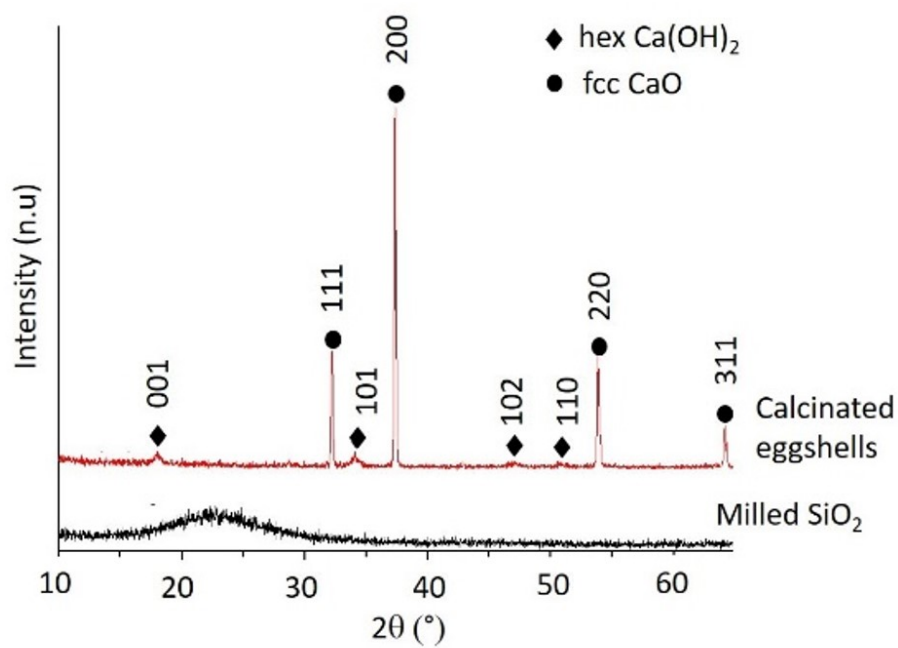


Figure 2. SEM images of starting materials. a) calcinated eggshells at 900°C for 12h, b) milled SiO₂ for 3h.



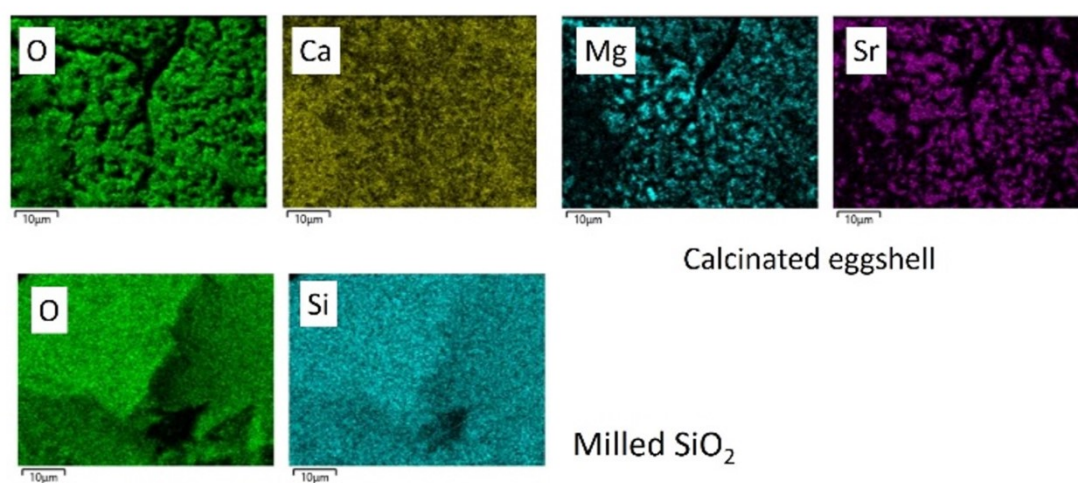
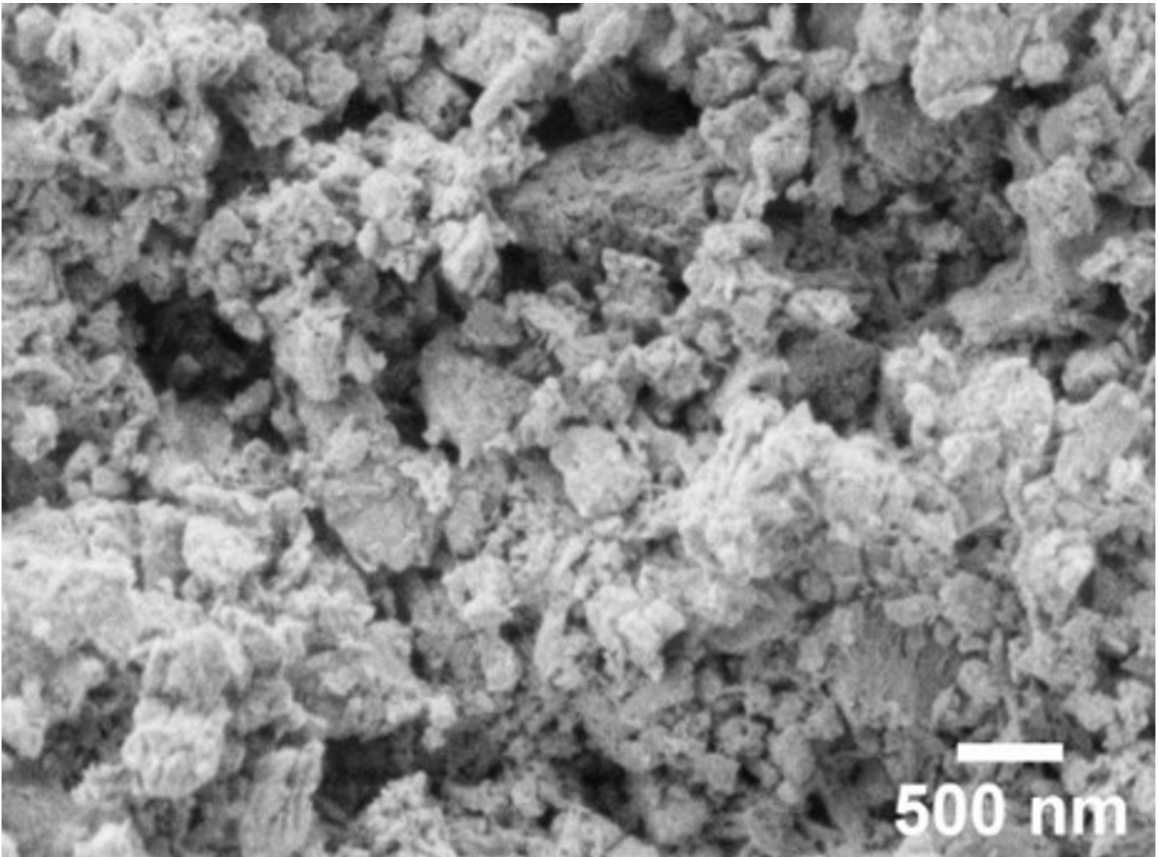
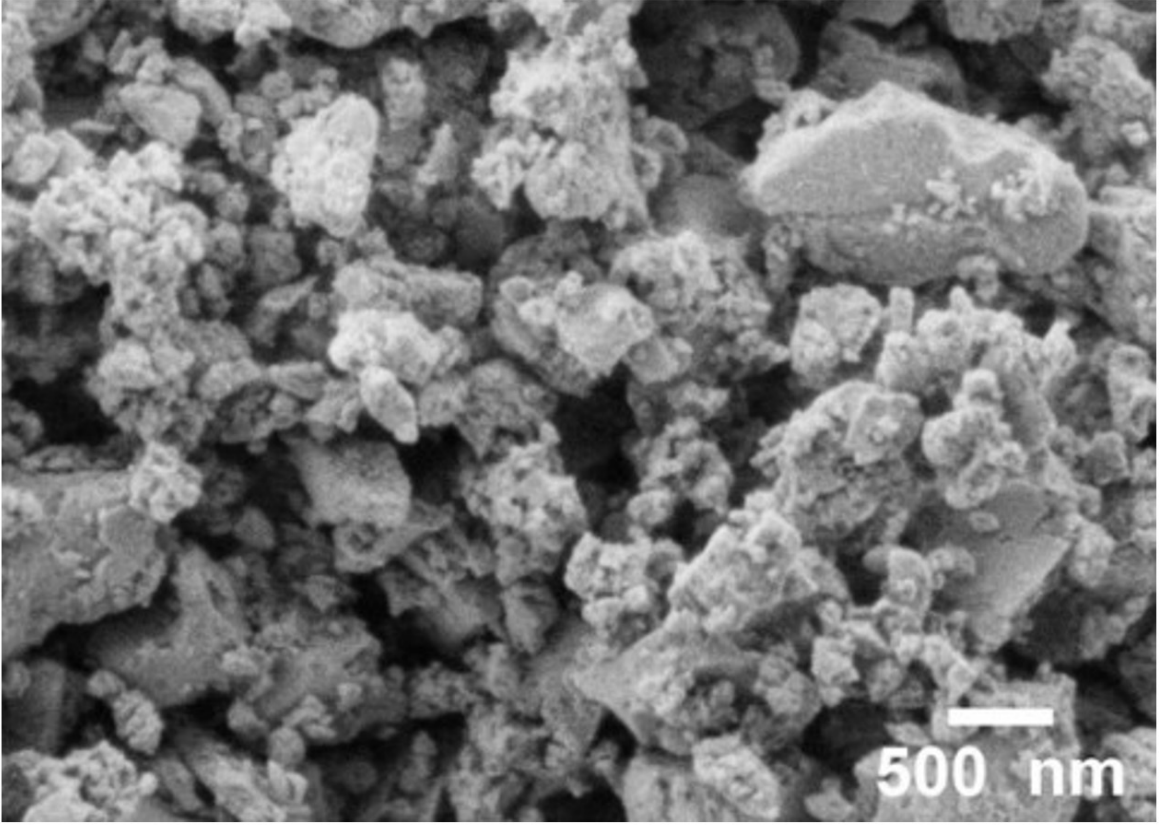


Figure 3. Phase and elemental analysis of the starting materials. a) XRD patterns, b) EDS elemental maps.



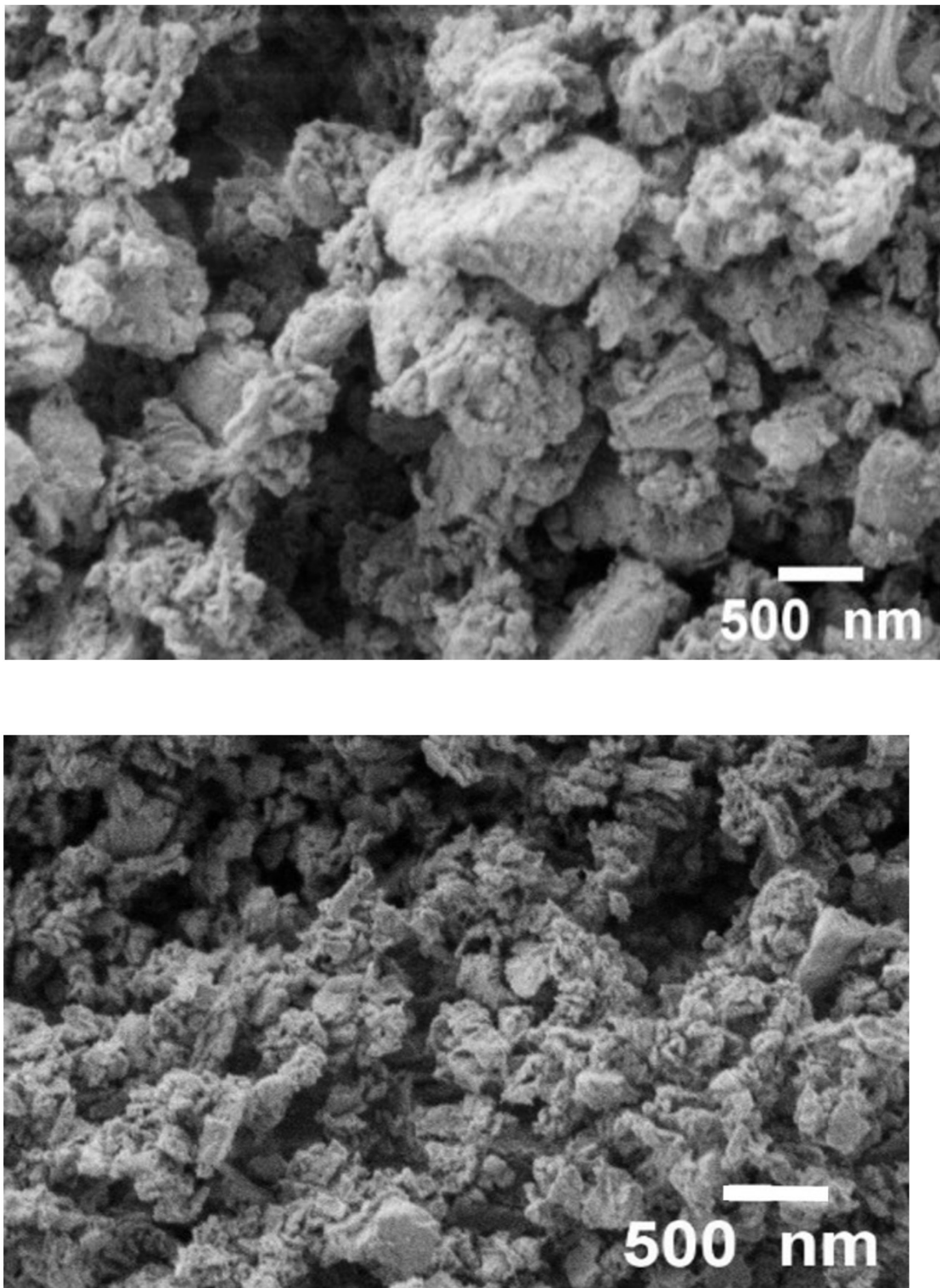


Figure 4. SEM images of different powder mixtures. a) 10C90S, b) 40C60S, c) 50C50S and d) 90C10S.

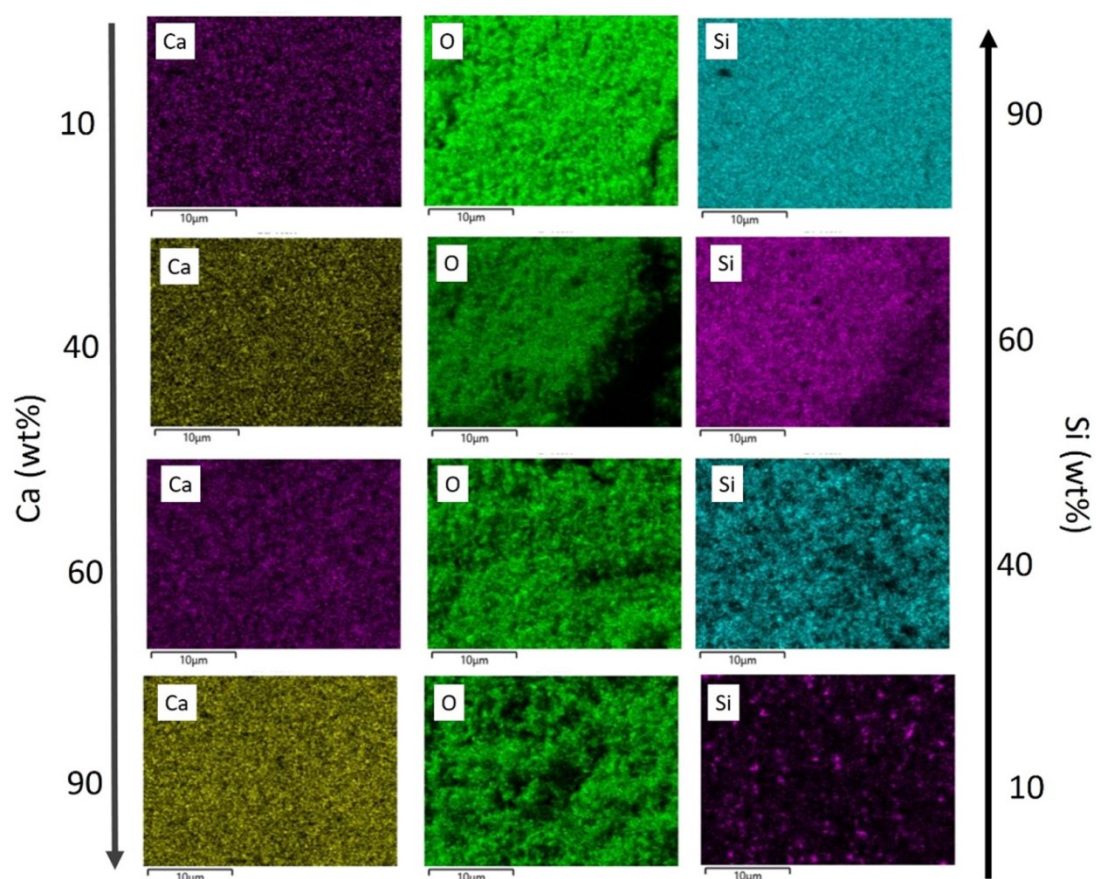


Figure 5. EDS measurements on different powder mixtures: 10C90S, 40C60S, 50C50S, 90C10S.

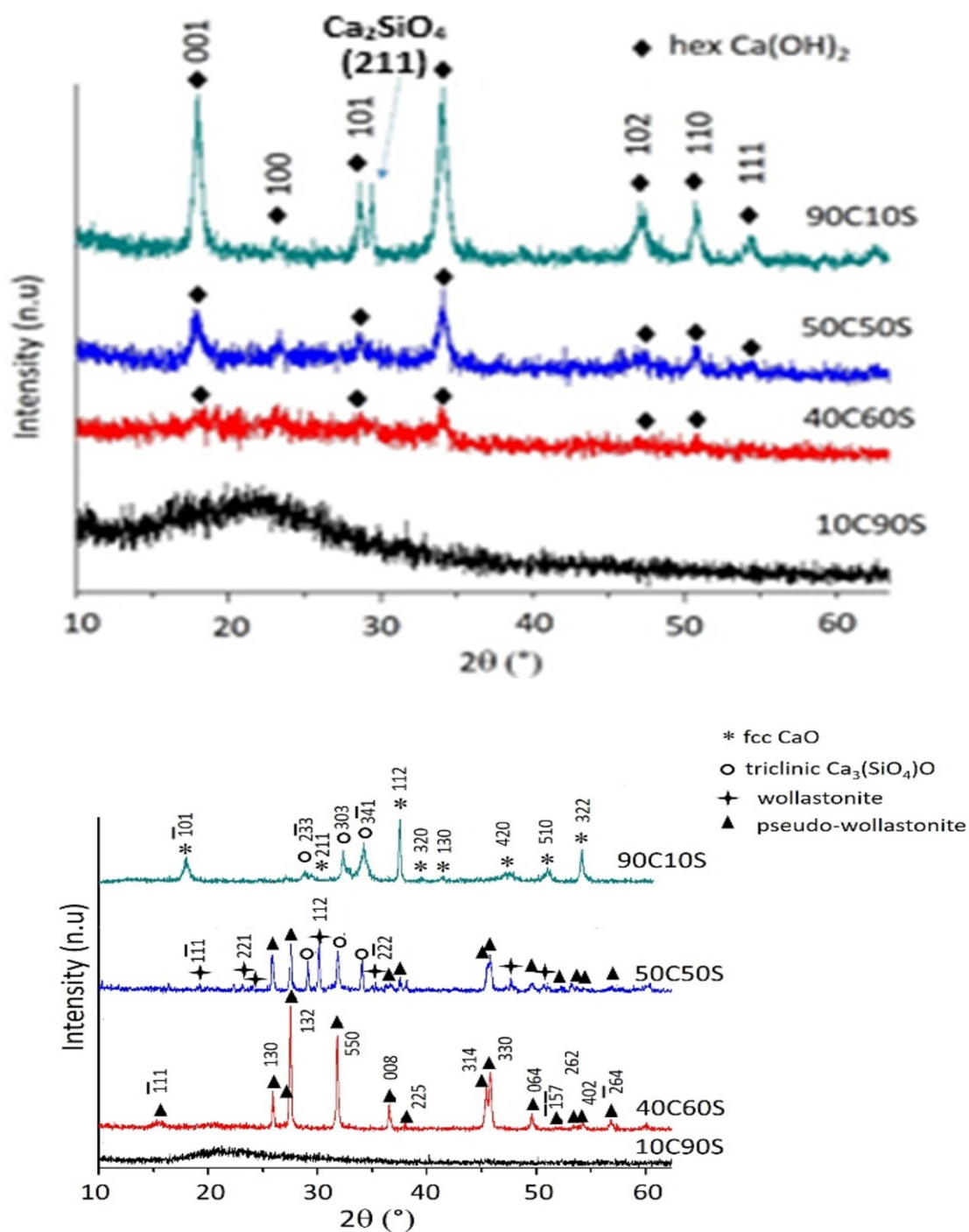
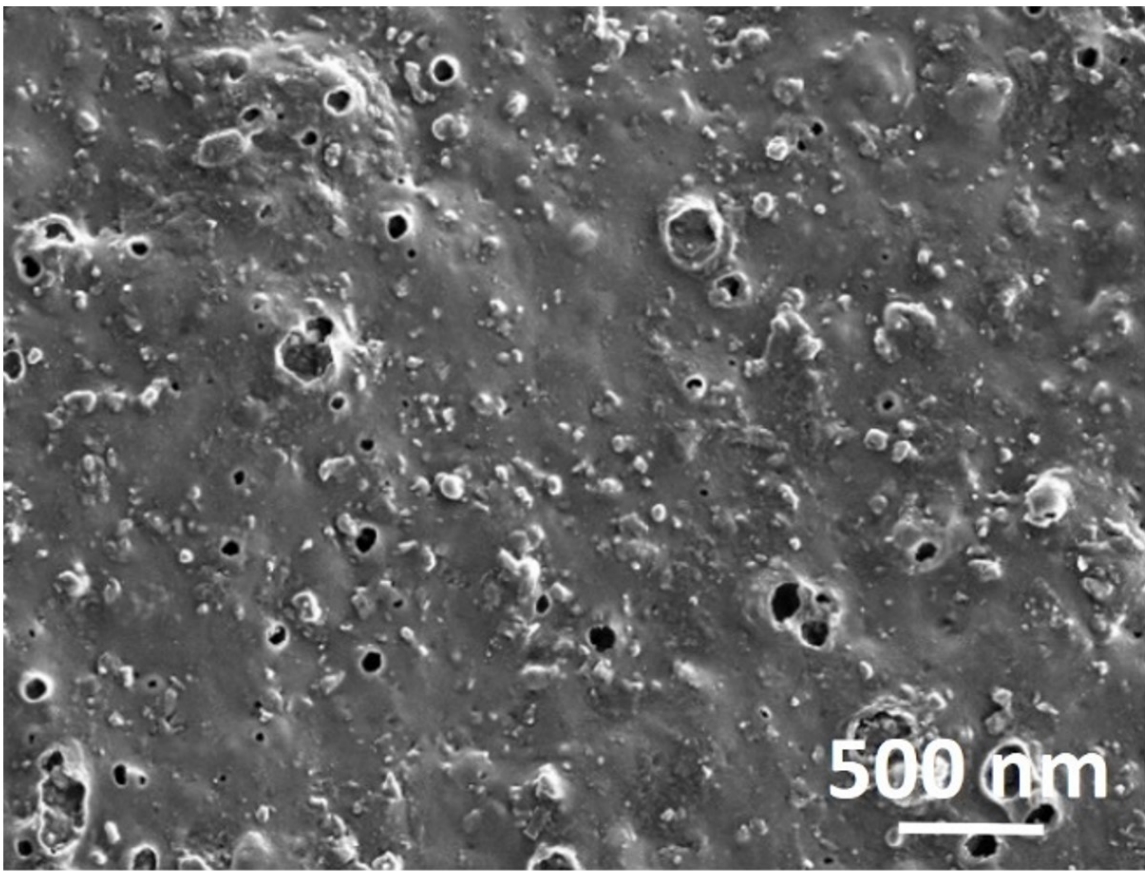
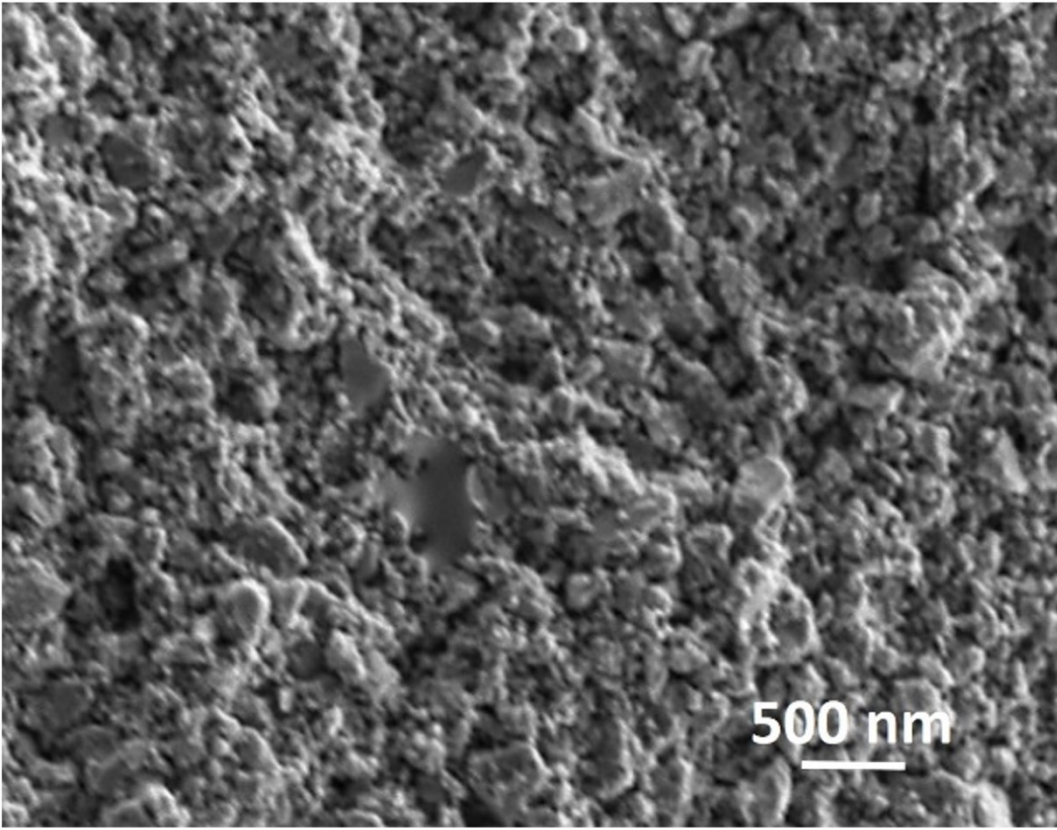


Figure 6. XRD patterns of calcium silica ceramics. a) powders with different composition, b) pressed and heat treated ceramics.



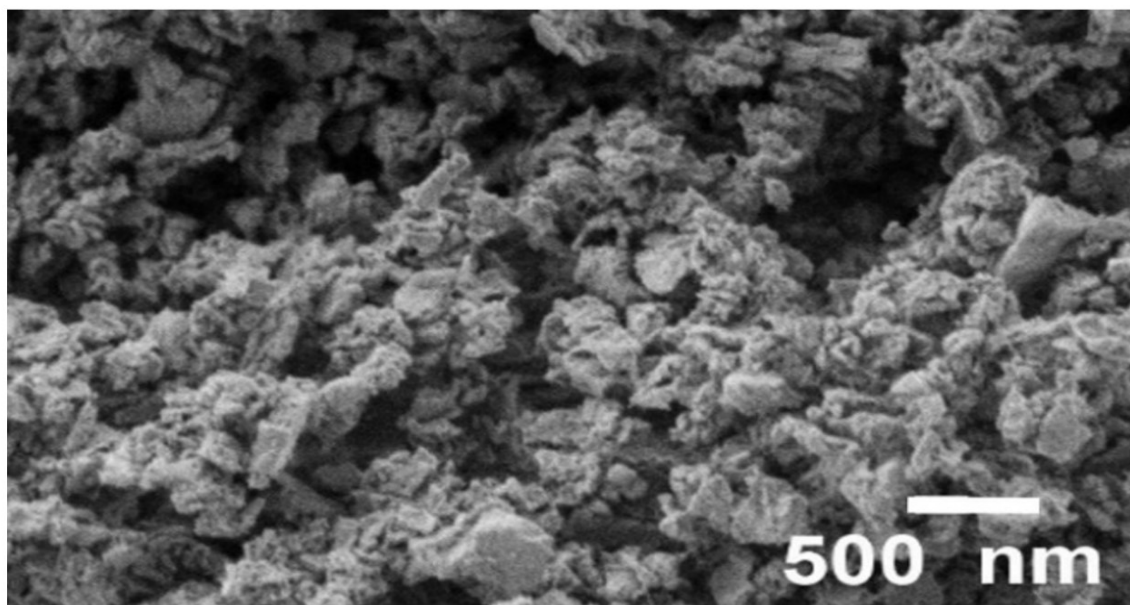
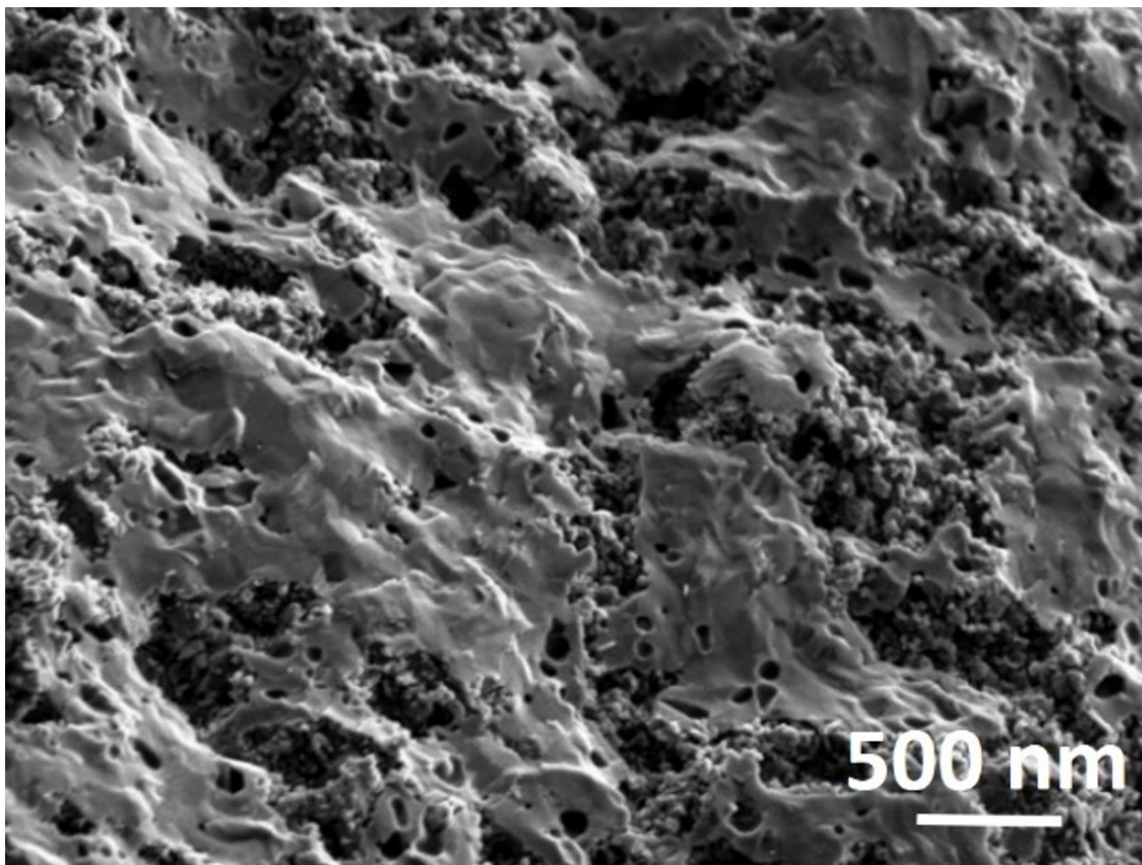


Figure 7. SEM images of pressed and heat treated ceramics with various composition. a) 10C90S, b) 40C60S, c) 50C50S and d) 90C10S.

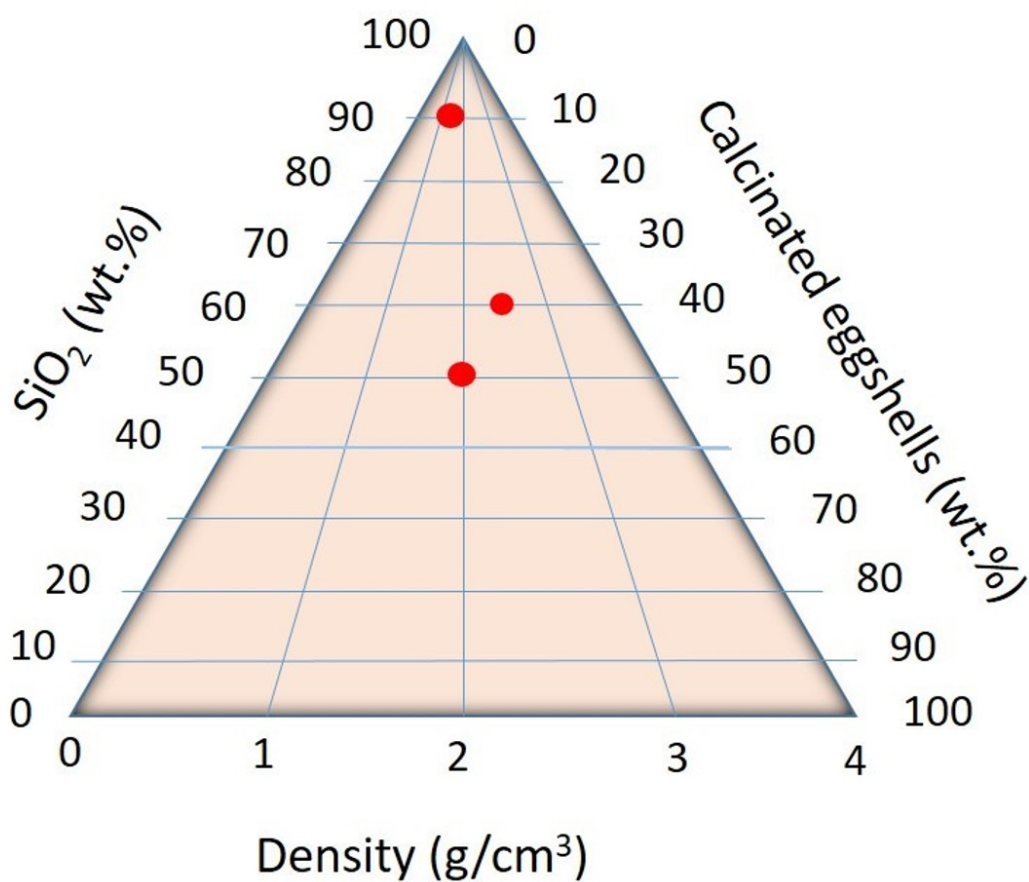
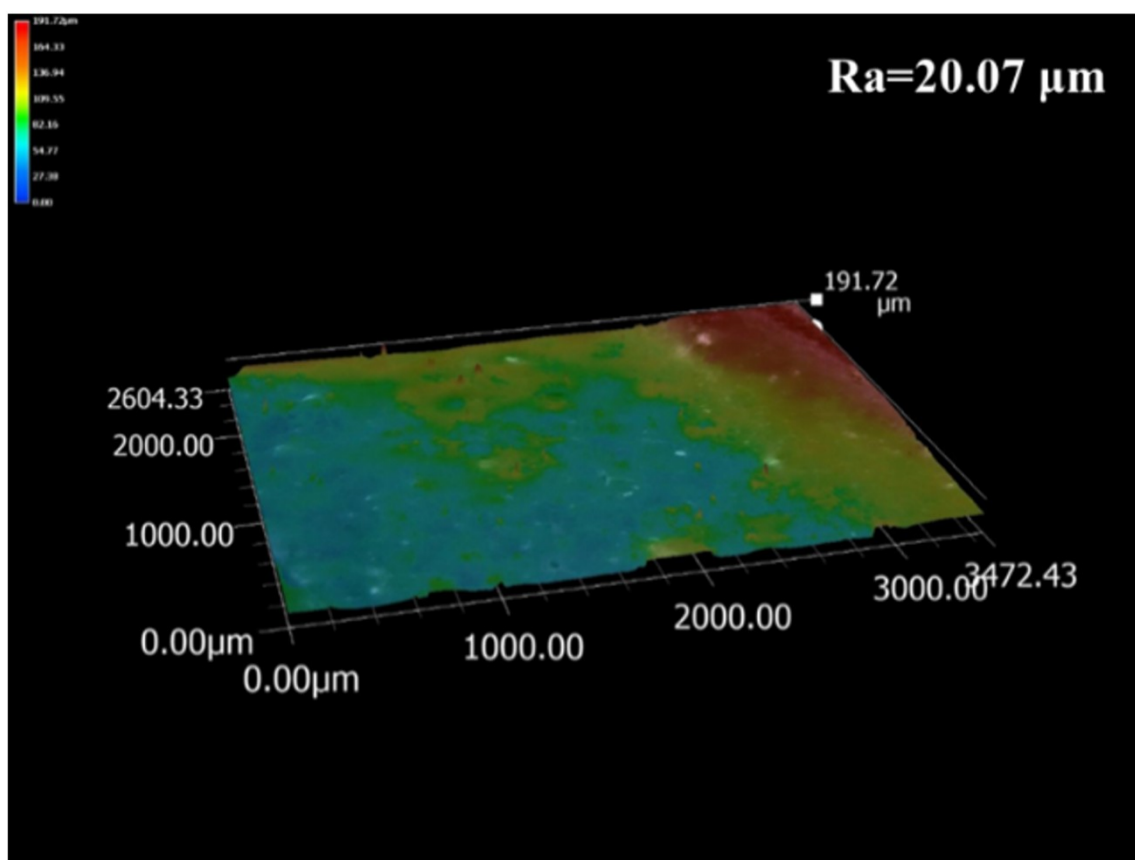
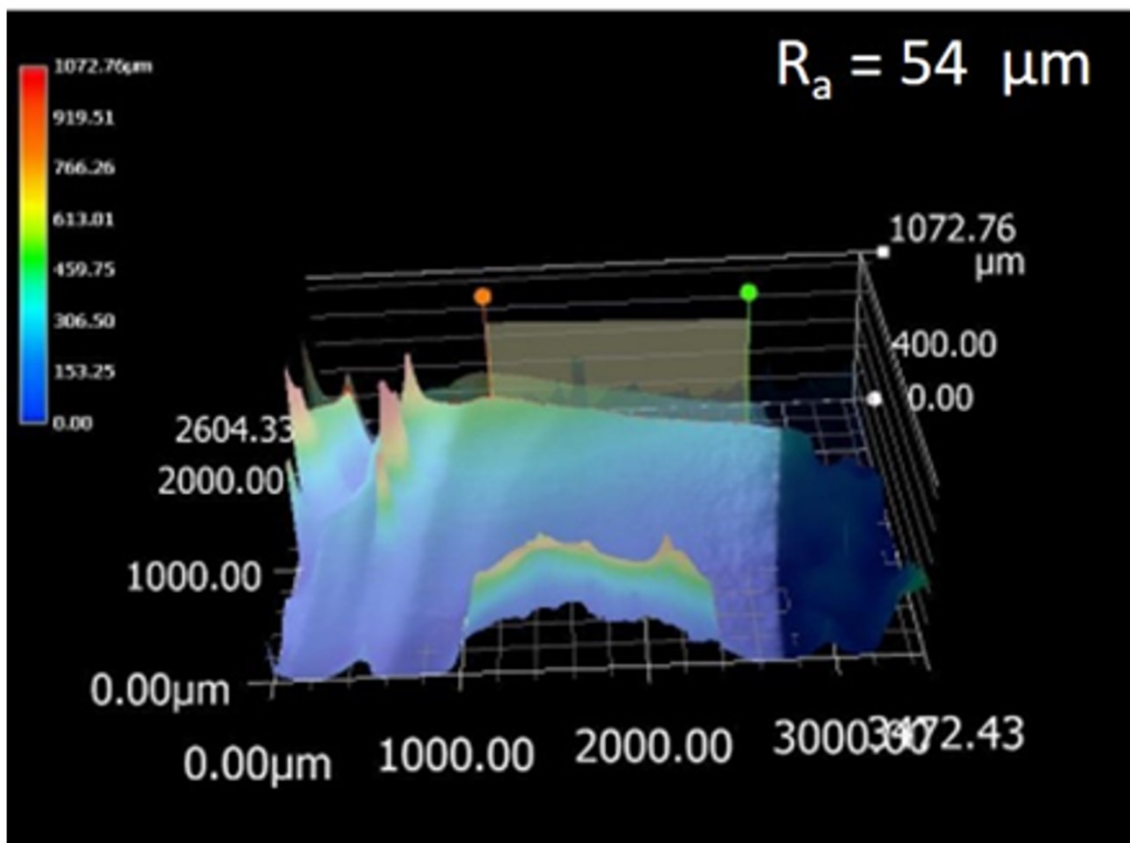


Figure 8. Density measurements for different compositions.* density of 90C10S was not measurable because of porous behavior.



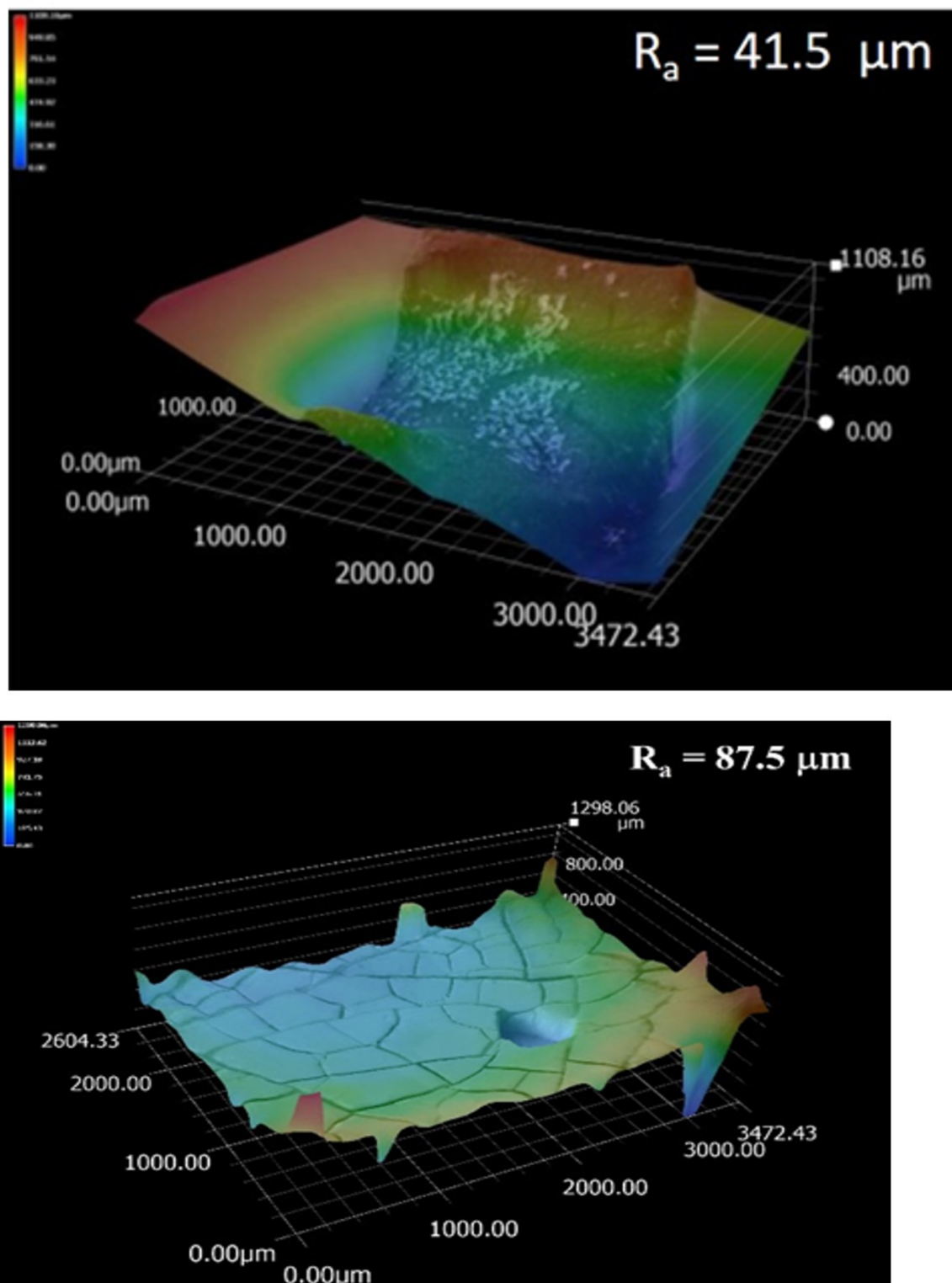


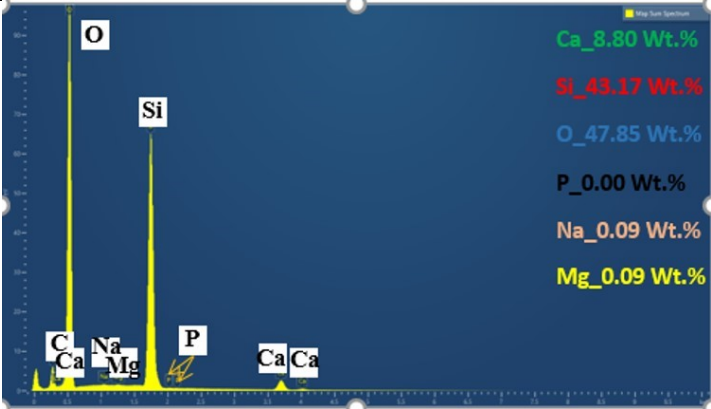
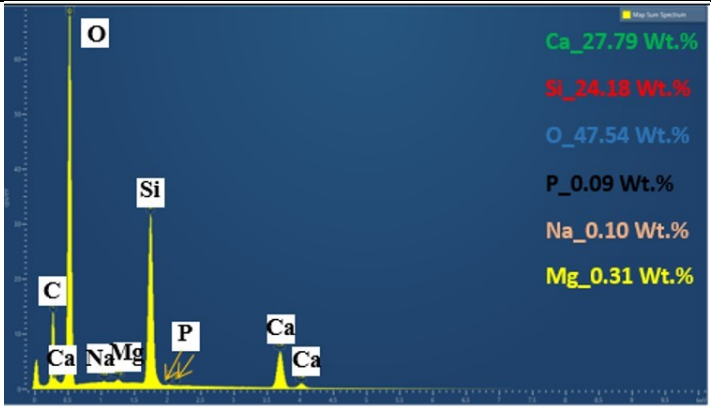
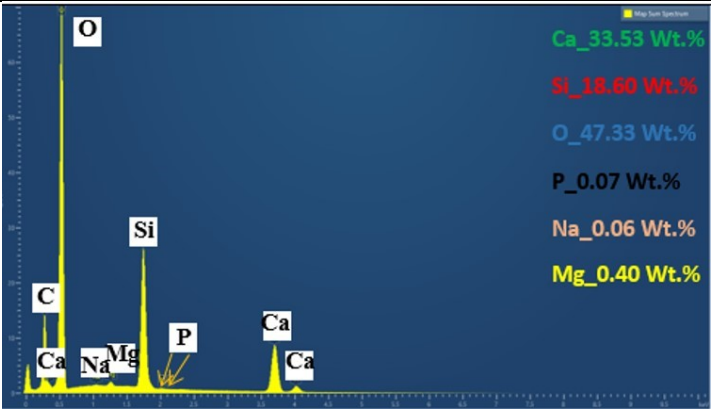
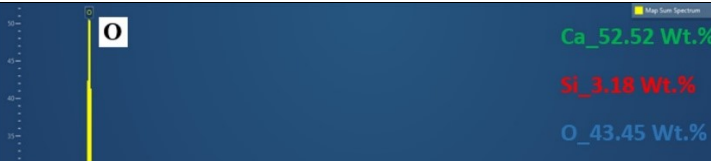
Figure 9. Roughness of the heat treated calcium silicates. a) 10C90S, b) 40C60S, c) 50S50C, d) 90C10S.

Table captions

Table 1. Different compositions and their notation.

Composition (wt%)	10C90S	40C60S	50C50S	90C10S
calcinated eggshell	10	40	50	90
milled SiO ₂	90	60	50	10

Table 2. EDS spectra with the atomic and weight percentages of elements for each powders

Composition	Elements and atomic (%)		EDS spectra with the weight percentage (Wt.%) of each element
10C90S	Ca	4.62	
	Si	32.33	
	O	62.90	
	Na	0.08	
	Mg	0.08	
	P	0.00	
40C60S	Ca	15.25	
	Si	18.94	
	O	65.33	
	Na	0.09	
	Mg	0.28	
	P	0.06	
50C50S	Ca	18.68	
	Si	14.79	
	O	66.05	
	Na	0.06	
	Mg	0.37	
	P	0.05	
90C10S	Ca	31.41	
	Si	2.71	

O	65.09
Na	0.07
Mg	0.52
P	0.19

Table 3. Weight, size changes before and after heat treatment and open porosities data of pressed ceramics.

Composition		10C90S	40C60S	50C50S	90C10S
weight (g)	before treatment	0.9467	0.9308	0.9381	0.9507
	after treatment	0.7214	0.6582	0.6851	0.7416
	Δw	- 0.2253	- 0.2726	- 0.2527	- 0.2091
diameter (mm)	before treatment	17.16	17.05	17.04	17.10
	after treatment	15.04	12.65	13.94	18.41
	Δd	- 2.12	- 4.4	- 3.1	+ 1.31